Research Article

Gian Paolo Beretta*, Luca Rivadossi, and Mohammad Janbozorgi

Systematic Constraint Selection Strategy for Rate-Controlled Constrained-Equilibrium Modeling of Complex Nonequilibrium Chemical Kinetics

An Automatable and Thermodynamically Consistent, Quasi-Equilibrium Model of Far Nonequilibrium States of Complex Reacting Systems Based on Probing the Fully Detailed Model and Taking a Truncated Singular Value Decomposition of the Resulting Evolution of the Degrees of Disequilibrium

https://doi.org/10.1515/jnet-2017-0055
Received September 28, 2017; revised February 8, 2018; accepted February 26, 2018

Abstract: Rate-Controlled Constrained-Equilibrium (RCCE) modeling of complex chemical kinetics provides acceptable accuracies with much fewer differential equations than for the fully Detailed Kinetic Model (DKM). Since its introduction by James C. Keck, a drawback of the RCCE scheme has been the absence of an automatable, systematic procedure to identify the constraints that most effectively warrant a desired level of approximation for a given range of initial, boundary, and thermodynamic conditions. An optimal constraint identification has been recently proposed. Given a DKM with S species, E elements, and R reactions, the procedure starts by running a probe DKM simulation to compute an S-vector that we call overall degree of disequilibrium (ODoD) because its scalar product with the S-vector formed by the stoichiometric coefficients of any reaction yields its degree of disequilibrium (DoD). The ODoD vector evolves in the same (S-E)-dimensional stoichiometric subspace spanned by the R stoichiometric S-vectors. Next we construct the rank-(S-E) matrix of ODoD traces obtained from the probe DKM numerical simulation and compute its singular value decomposition (SVD). By retaining only the first C largest singular values of the SVD and setting to zero all the others we obtain the best rank-C approximation of the matrix of ODoD traces whereby its columns span a C-dimensional subspace of the stoichiometric subspace. This in turn yields the best approximation of the evolution of the ODoD vector in terms of only C parameters that we call the constraint potentials. The resulting order-C RCCE approximate model reduces the number of independent differential equations related to species, mass, and energy balances from S+2 to C+E+2, with substantial computational savings when $C \ll S\text{-}E$.

Keywords: model reduction in nonequilibrium thermodynamics, rate-controlled constrained equilibrium, RCCE constraints, degrees of disequilibrium, singular value decomposition, principal component analysis

Dedicated to the memory of James C. Keck, inventor of the RCCE approach; see www.JamesKeckCollectedWorks.org

1 Introduction

Various techniques for model order reduction in chemical kinetics and dynamical systems hinge on the time separation between a subset of "relatively fast" kinetic mechanisms that contribute rapidly to the system's partial equilibration and a subset of "bottleneck" mechanisms that effectively control and slow down the

***Corresponding author: Gian Paolo Beretta,** Dept. of Mech. and Industrial Eng. (DIMI), Università di Brescia, Brescia, Italy, e-mail: gianpaolo.beretta@unibs.it
Luca Rivadossi, Dept. of Mech. and Industrial Eng. (DIMI), Università di Brescia, Brescia, Italy, e-mail: luca.rivadossi@alice.it
Mohammad Janbozorgi, Dept. of Mech. and Aerospace Eng. (MAE), University of California, Los Angeles, CA, USA, e-mail: mjanbozorgi@gmail.com

relaxation towards complete equilibrium. For example in the kinetic theory of gases, three-body collisions – which occur much less frequently than two-body collisions – form a subset of bottleneck mechanisms which for sufficient dilution can even be neglected (such as in the standard Boltzmann equation), whereas for denser gases they are the slow rate-controlling mechanisms. For the same reason, in chemical kinetics the three-body reactions are slow and almost always among the rate-controlling bottleneck mechanisms: the associated rate-limiting constraint is the total number of moles, which would be conserved in the absence of three-body reactions.

When modeling the nonequilibrium dynamics of systems such as turbulent combustion of heavy hydrocarbon fuels, where the transport of hundreds of chemical species must be considered together with the kinetics of thousands of chemical reactions, model order reduction techniques are essential for effective numerical simulation and several methods have been developed over the past several decades. It is not our purpose here to review the vast and growing literature on the subject by various independent research groups (see, e. g., Refs. [1, 2, 3, 4, 5, 6, 7, 8, 9, 10, 11, 12, 13, 14, 15, 16] and the many more references cited therein and citing these papers thereafter). In this paper we focus on the RCCE approach [4, 5, 16, 17, 18, 19, 20] and present a possible strategy to resolve a long standing problem that has so far prevented its widespread systematic application in spite of its strong built-in thermodynamic consistency.

Chemical kinetic models are usually characterized by a wide spectrum of time scales. In recent years the same techniques are being developed and adapted to tackle also large-scale models of cellular reaction networks and complex models that account for many details of the physiology, biochemistry, and genetics of cell cycle control, such as in budding yeast modeling [21, 22, 23].

For each particular problem, set of conditions, and acceptable degree of approximation the RCCE approach to modeling the nonequilibrium dynamics is based on assuming that: (1) there is a threshold time scale which essentially separates the "relatively fast" equilibrating kinetic mechanisms from the "relatively slow" ones; (2) if the latter were frozen the system would be characterized by an additional set of conserved properties, called RCCE constraints; (3) at any time and every spatial position the local nonequilibrium state is well approximated by the partial equilibrium state which maximizes the entropy density subject to the local density values of the set of conserved properties augmented by the RCCE constraints. The RCCE constraints characterize the bottlenecks of the kinetic scheme that for the time scale of interest essentially characterize the "relatively slow" and hence interesting part of the nonequilibrium dynamics. As long as the RCCE constraints can be assumed fixed, the RCCE constraints identify a low-dimensional manifold in composition space, where the time evolution can be assumed to take place for the chosen level of approximation.

As emphasized for example in Ref. [16], the main difficulty in the practical implementation of the RCCE modeling approach has been the lack of a systematic method for identifying the kinetic bottlenecks and the corresponding set of constraints. Several efforts have addressed these problems with varying degrees of success (see, e. g., Refs. [24, 25, 26, 27, 28, 29, 30, 31, 32, 33] and references therein). Below, the constraint selection strategy we proposed in Ref. [34] is reformulated and illustrated by means of abstract geometric considerations that may help establish connections with the more general nonequilibrium thermodynamics frameworks discussed in Refs. [35, 36, 37, 38, 39, 40, 41] and references therein.

2 Standard DKM formulation

A Detailed Kinetic Model (DKM) for gas-phase combustion with $n_{\rm sp}$ chemical species and $n_{\rm r}$ reactions is typically defined by the following set of assumptions. The terms $\nu_{j\ell}^{+}$ and $\nu_{j\ell}^{-}$ denote the forward and reverse stoichiometric coefficients of species j in reaction ℓ. The kinetic parameters A_ℓ^+, b_ℓ^+, and E_ℓ^+ determine the forward reaction rate constants $k_\ell^+(T) = A_\ell^+\, T^{b_\ell^+}\, \exp(-E_\ell^+/RT)$ (typically in mol-cm-s-K units with the forward activation energy E_l^+ in cal/mol). The principle of detailed balance determines the backward reaction rate constants according to $k_\ell^-(T) = k_\ell^+(T)\, K_\ell^{\rm co}(T)$, where the equilibrium constant based on concentrations is $K_\ell^{\rm co}(T) = (p_o/RT)^{\nu_\ell}\, \exp(-\Delta g_\ell^o(T)/RT)$ with $\nu_\ell = \sum_{j=1}^{n_{\rm sp}} (\nu_{j\ell}^- - \nu_{j\ell}^+)$ and $\Delta g_\ell^o(T) = \sum_{j=1}^{n_{\rm sp}} \nu_{j\ell}\, g_{j,{\rm pure}}(T, p_o)$ (Gibbs free energy of reaction ℓ at standard pressure p_o and temperature T).

Here, we use the notation of [16], which differs only slightly from that of [42], whereby $g_{j,\mathrm{pure}} = \mu_{j,\mathrm{pure}}$ refers to the Gibbs free energy of pure species j, whereas the symbol $g_j = \mu_j$ represents the partial Gibbs free energy, i. e., the chemical potential, of species j in the mixture.

Forward and reverse reaction rates, r_ℓ^+ and r_ℓ^-, are given by $r_\ell^\pm = k_\ell^\pm(T)\prod_{j=1}^{n_{\mathrm{sp}}}[N_j]^{\nu_{j\ell}^\pm}$ where $[N_j]$ is the concentration of species j. These in turn determine the chemical production density terms in the species balance equations (consumption density if negative) $\omega_j = \sum_{\ell=1}^{n_{\mathrm{r}}}\nu_{j\ell}(r_\ell^+ - r_\ell^-)$ and the chemical contribution to the entropy production density $\sigma_{\mathrm{chem}} = R\sum_{\ell=1}^{n_{\mathrm{r}}}(r_\ell^+ - r_\ell^-)\ln(r_\ell^+/r_\ell^-)$.

The local-equilibrium simple-system assumption assigns to the local fluid element the properties of the so-called "surrogate system" [42], i. e., of the stable thermodynamic equilibrium state of a nonreacting ("frozen") mixture with the same energy and composition of the fluid element, under the assumption of an ideal Gibbs–Dalton mixture of ideal gases, whereby $p = [N]RT$ and the chemical potentials are related to the mole fractions X_j by $\mu_j(T,p,\boldsymbol{X}) = g_{j,\mathrm{pure}}(T,p_o) + RT\ln(p/p_o) + RT\ln(X_j)$.

3 RCCE model of local nonequilibrium states

The RCCE method models the local nonequilibrium states as partially equilibrated states with the local mole fractions $X_j^{\mathrm{CE}} = N_j/\sum_{k=1}^{n_{\mathrm{sp}}}N_k$ (where N_j represents the molar amount of species j) that minimize the Gibbs free energy subject to the local values of temperature T, pressure p, and molar amounts of elements $N_i^{\mathrm{EL}} = \sum_{j=1}^{n_{\mathrm{sp}}}a_{ij}^{\mathrm{EL}}N_j = \langle \boldsymbol{a}_i^{\mathrm{EL}}|\boldsymbol{N}\rangle$ (where a_{ij}^{EL} represents the number of atoms of element i in a molecule of species j, $\boldsymbol{a}_i^{\mathrm{EL}}$ its row entries arranged in an n_{sp}-dimensional vectors, $\boldsymbol{N}$ the species amounts arranged in an n_{sp}-dimensional vector, and $\langle\cdot|\cdot\rangle$ the scalar product in $\mathbb{R}^{n_{\mathrm{sp}}}$) and to the local values of a set of n_c slowly varying and, hence, rate-controlling constraints assumed to be given by linear combinations of the molar amounts, i. e., $c_i(\boldsymbol{N}) = \sum_{j=1}^{n_{\mathrm{sp}}}a_{ij}^{\mathrm{CE}}N_j = \langle \boldsymbol{a}_i^{\mathrm{CE}}|\boldsymbol{N}\rangle$, where the matrix a_{ij}^{CE} (with its row entries arranged in the n_{sp}-dimensional vectors $\boldsymbol{a}_i^{\mathrm{CE}}$) is the heart of the model in that it is assumed to fully characterize the rate-controlling bottlenecks of the full kinetic mechanism all along the evolution of interest, i. e., to remain fixed during the evolution. For ideal gas mixture behavior, i. e., chemical potentials given by $\mu_j(T,p,\boldsymbol{X}) = g_{j,\mathrm{pure}}(T,p) + RT\ln X_j$, the constrained maximization yields the composition

$$\ln X_j^{\mathrm{CE}} = -g_{j,\mathrm{pure}}(T,p)/RT - \sum_{i=1}^{n_{\mathrm{el}}}\gamma_i^{\mathrm{EL}}a_{ij}^{\mathrm{EL}} - \sum_{i=1}^{n_{\mathrm{c}}}\gamma_i^{\mathrm{CE}}a_{ij}^{\mathrm{CE}}, \tag{1}$$

that is,

$$\Lambda_j \equiv -\frac{1}{RT}\mu_j(T,p,\boldsymbol{X}^{\mathrm{CE}}) = \sum_{i=1}^{n_{\mathrm{el}}}\gamma_i^{\mathrm{EL}}a_{ij}^{\mathrm{EL}} + \sum_{i=1}^{n_{\mathrm{c}}}\gamma_i^{\mathrm{CE}}a_{ij}^{\mathrm{CE}}, \tag{2}$$

where we denote by $\Lambda_j = \mu_j/RT$ the (dimensionless) entropic chemical potentials. The Lagrange multipliers γ_i^{EL} and γ_i^{CE} are called elemental and constraint potentials, respectively. For the ℓth chemical reaction $\sum_{j=1}^{n_{\mathrm{sp}}}\nu_{j\ell}A_j = 0$, the stoichiometric balance requires $b_{i\ell}^{\mathrm{EL}} = \sum_{j=1}^{n_{\mathrm{sp}}}a_{ij}^{\mathrm{EL}}\nu_{j\ell} = \langle \boldsymbol{a}_i|\boldsymbol{\nu}_\ell\rangle = 0$, where $\boldsymbol{\nu}_\ell$ are the column entries of the matrix of stoichiometric coefficients $\nu_{j\ell}$ arranged in n_{sp}-dimensional vectors. The advantage of the RCCE approximation is that the composition depends only on the $n_{\mathrm{el}} + n_{\mathrm{c}}$ parameters γ_i^{EL} and γ_i^{CE}, instead of the n_{sp} molar amounts of species which can be many more. In the CFD modeling contexts (for example of flame propagation in internal combustion engines [43]), this means that in addition to the continuity, Navier–Stokes, and energy balance equations, the n_{sp} species balance equations can be effectively substituted by the $n_{\mathrm{el}} + n_{\mathrm{c}}$ balance equations for the elemental and constraint potentials (see eqs. (10)–(14) below), thus achieving a substantial model reduction that has a built-in strong thermodynamic consistency and does not require to cut the number of species nor the number of reactions to be taken into account. The method has been used with excellent results when a proper choice of constraints is made. For example (see, e. g., [44, 45]) for the ignition delay of hydrogen–oxygen mixtures ($n_{\mathrm{sp}} = 8$, $n_{\mathrm{el}} = 2$), the RCCE method yields excellent agreement with fully detailed model predictions by using only $n_{\mathrm{c}} = 2$ constraints, with a saving of $8 - (2 + 2) = 4$ differential equations. The computational savings is much more important for higher hydrocarbons, for example,

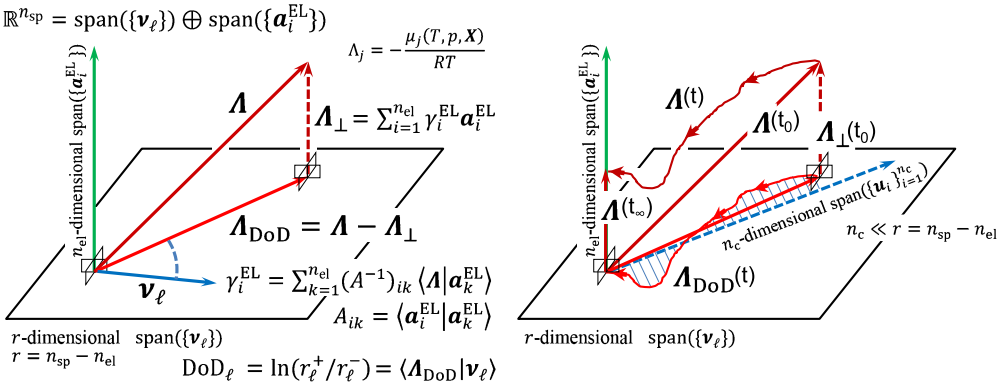

Figure 1: Left: Pictorial representation of the projection that defines the overall DoD vector $\boldsymbol{\Lambda}_{DoD}$ from the vector $\boldsymbol{\Lambda}$ of the entropic potentials, showing their geometric relations with the DoD's ϕ_ℓ (scalar product between $\boldsymbol{\Lambda}_{DoD}$ and the stoichiometric vector $\boldsymbol{\nu}_\ell$ of reaction ℓ) and the elemental constraint potentials γ_i^{EL} (in terms of the row vectors $\boldsymbol{a}_i^{EL}$ of the elemental composition matrix a_{ij}^{EL}). Here $\boldsymbol{\Lambda}_\perp$ is shorthand for $\boldsymbol{\Lambda}_{\mathrm{span}(\{\boldsymbol{a}_i^{EL}\})}$. **Right:** Pictorial representation of the projection of a time-dependent trajectory $\boldsymbol{\Lambda}_{DoD}(t)$ for a relaxation transient and its "closest" n_c-dimensional subspace, $\mathrm{span}(\{\boldsymbol{u}_{i=1}^{n_c}\})$, identified by the n_c-truncated SVD of the discretized path $\boldsymbol{\Lambda}_\perp(t)$ obtained from the solution of a full DKM probe computation.

for methane–oxygen ignition ($n_{sp} = 29$, $n_{el} = 3$) excellent results [44, 45] are obtained with $n_c = 13$, with a saving of $29 - (3 + 13) = 13$ differential equations and without giving up the ability to predict fine details such as the typical temperature and composition overshoots occurring immediately following ignition.

4 ASVDADD strategy for identifying optimal RCCE constraints

The recently proposed algorithm based on Approximate Singular Value Decomposition of the Actual Degrees of Disequilibrium (ASVDADD) [34] allows the identification of optimal sets of constraints with no need for deep knowledge and understanding of chemical kinetics fundamentals such as chain branching, radical formation, etc., thus making the RCCE method accessible to a broad range of scientists and engineers. The algorithm is based on the following basic observations. The degree of disequilibrium (DoD) of reaction ℓ, defined by $\phi_\ell = \ln r_\ell^+ / r_\ell^-$, is given in general by

$$\phi_\ell = \ln \frac{r_\ell^+}{r_\ell^-} = -\frac{1}{RT} \sum_{j=1}^{n_{sp}} \mu_j \nu_{j\ell} = \sum_{j=1}^{n_{sp}} \Lambda_j \nu_{j\ell} = \langle \boldsymbol{\Lambda} | \boldsymbol{\nu}_\ell \rangle. \tag{3}$$

The entropic chemical potentials Λ_j can be viewed as the components of the n_{sp}-vector $\boldsymbol{\Lambda}$. Also the n_{el} rows of the elemental composition matrix a_{ij}^{EL} can be viewed as the components of the n_{sp}-vectors $\boldsymbol{a}_i^{EL}$. Due to the orthogonality relation $\sum_{j=1}^{n_{sp}} a_{ij}^{EL} \nu_{j\ell} = \langle \boldsymbol{a}_i | \boldsymbol{\nu}_\ell \rangle = 0$, the n_{el}-dimensional linear span of vectors $\boldsymbol{a}_i^{EL}$ is the left null space of the matrix $\nu_{j\ell}$ of stoichiometric coefficients, often called the inert subspace. In view of its orthogonality with the inert subspace, the $(n_{sp} - n_{el})$-dimensional linear span($\{\boldsymbol{\nu}_\ell\}$) is usually called the stoichiometric subspace or reactive subspace. As illustrated pictorially in Fig. 1 (left), the projection of vector $\boldsymbol{\Lambda}$ onto the inert subspace can be written as $\boldsymbol{\Lambda}_\perp = \boldsymbol{\Lambda}_{\mathrm{span}(\{\boldsymbol{a}_i^{EL}\})} = \sum_{i=1}^{n_{el}} \gamma_i^{EL} \boldsymbol{a}_i^{EL}$, where the coefficients γ_i^{EL} can be readily computed: $\gamma_i^{EL} = \sum_{k=1}^{n_{el}} (A^{-1})_{ik} \langle \boldsymbol{\Lambda} | \boldsymbol{a}_k^{EL} \rangle$, where A^{-1} is the inverse of the matrix with elements $A_{ik} = \langle \boldsymbol{a}_i^{EL} | \boldsymbol{a}_k^{EL} \rangle$ (for a proof see, e. g., the appendix of Ref. [46]). Since $\boldsymbol{\Lambda}_{\mathrm{span}(\{\boldsymbol{a}_i^{EL}\})}$ does not contribute to the DoD of any reaction (in fact, $\sum_{j=1}^{n_{sp}} \sum_{i=1}^{n_{el}} \gamma_i^{EL} a_{ij}^{EL} \nu_{j\ell} = \sum_{i=1}^{n_{el}} \gamma_i^{EL} b_{i\ell}^{EL} = 0$), we call the vector

$$\boldsymbol{\Lambda}_{DoD} = \boldsymbol{\Lambda} - \boldsymbol{\Lambda}_{\mathrm{span}(\{\boldsymbol{a}_i^{EL}\})} = \boldsymbol{\Lambda} - \sum_{i=1}^{n_{el}} \gamma_i^{EL} \boldsymbol{a}_i^{EL} \quad \text{or, equivalently,} \quad \Lambda_{DoD,j} = \Lambda_j - \sum_{i=1}^{n_{el}} \gamma_i^{EL} a_{ij}^{EL} \tag{4}$$

the "overall DoD vector." In fact, eq. (3) shows that it contains the information about the DoDs, ϕ_ℓ, of all the reactions. It is the null vector if and only if they are all equilibrated, i. e., only for the chemical equilibrium states. Notice that within the RCCE model, from eq. (1), we have

$$\mathbf{\Lambda}^{\mathrm{RCCE}}_{\mathrm{DoD}} = \sum_{i=1}^{n_{\mathrm{c}}} \gamma_i^{\mathrm{CE}}\, \boldsymbol{a}_i^{\mathrm{CE}} \quad \text{or, equivalently,} \quad \Lambda^{\mathrm{RCCE}}_{\mathrm{DoD},j} = \sum_{i=1}^{n_{\mathrm{c}}} \gamma_i^{\mathrm{CE}}\, a_{ij}^{\mathrm{CE}}. \tag{5}$$

Since the $\boldsymbol{a}_i^{\mathrm{CE}}$ vectors are assumed to be fixed for a (given portion of a) given evolution, eq. (5) shows that the overall DoD vector remains within the subspace span $\left(\{\boldsymbol{a}_i^{\mathrm{CE}}\}_{i=1}^{n_{\mathrm{c}}}\right)$ for the entire (portion of the) evolution. Within the RCCE model, therefore, this subspace can be viewed as a low-dimensional slow invariant manifold (LDSIM) (see, e. g., [7, 9, 11, 47, 48, 49] and references therein) although it is not an invariant manifold of the full DKM.

Now let us consider a CFD numerical simulation in which the index $z = 1, \ldots, Z$ labels the space–time discretization (i. e., z labels both the finite volumes or elements of the mesh as well as the time grid). If we adopt the full DKM and solve the full set of balance equations including those for all the species, the resulting overall DoD vectors form an $n_{\mathrm{sp}} \times Z$ matrix $\Lambda^{\mathrm{DKM}}_{\mathrm{DoD},jz} = \Lambda_{\mathrm{DoD},j}(z)$ that has rank $r = n_{\mathrm{sp}} - n_{\mathrm{el}}$. If instead the local states are described according to the RCCE assumption defined above, the $n_{\mathrm{sp}} \times Z$ matrix $\Lambda^{\mathrm{RCCE}}_{\mathrm{DoD},jz} = \Lambda^{\mathrm{RCCE}}_{\mathrm{DoD},j}(z) = \sum_{i=1}^{n_{\mathrm{c}}} \gamma_i^{\mathrm{CE}}(z)\, a_{ij}^{\mathrm{CE}}$ has a rank equal to the (typically much smaller) number n_{c} of constraints. In other words, even if the number n_{sp} of chemical species in the underlying DKM is in the hundreds and therefore the $n_{\mathrm{sp}} \times Z$ overall DoD matrix $\Lambda^{\mathrm{DKM}}_{\mathrm{DoD},jz}$ has rank $n_{\mathrm{sp}} - n_{\mathrm{el}}$, its approximation within the RCCE model, $\Lambda^{\mathrm{RCCE}}_{\mathrm{DoD},jz}$, is of the much lower rank n_{c}.

In order to identify the matrix a_{ij}^{CE} of the constraints that allow such approximation, the idea behind the ASVDADD algorithm is to probe the DKM by running a preliminary full DKM computation, possibly on a submesh of the full problem and for a shorter time so as to span a limited range of temperatures, pressures, and compositions. From such computation we obtain the $n_{\mathrm{sp}} \times Z$ overall DoD matrix, that we shall now denote for brevity by D, with elements $D_{jz} = \Lambda^{\mathrm{DKM}}_{\mathrm{DoD},jz}$. Then we compute its singular value decomposition (SVD). As is well known [50], the result can be written formally in reduced form as $D = U\, \mathrm{diag}(\boldsymbol{\sigma})\, V^T$, where U is an $n_{\mathrm{sp}} \times r$ orthogonal matrix (in the sense that $U^T U = I$, i. e., U^T is its left inverse) whose r columns form the vectors $|\boldsymbol{u}_i\rangle$ which represent an orthonormal basis for the column space of D, V^T is the transpose of a $Z \times r$ orthogonal matrix whose r column vectors $\boldsymbol{v}_i$ represent an orthonormal basis for the column space of D^T, and $\boldsymbol{\sigma}$ is an r-dimensional vector whose entries are the singular values of D arranged in decreasing order. Recalling that $r = \mathrm{rank}(D) = n_{\mathrm{sp}} - n_{\mathrm{el}}$, the SVD of the overall DoD matrix can be written explicitly as

$$D_{jz} = \Lambda^{\mathrm{DKM}}_{\mathrm{DoD},jz} = \sum_{i=1}^{r} U_{ji}\, \sigma_i\, V_{iz} = \sum_{i=1}^{r} U_{ji}\, \gamma_{iz}^{\mathrm{DKM}}, \tag{6}$$

where $\sigma_1 \geq \sigma_2 \geq \cdots \geq \sigma_r > 0$ and we defined $\gamma_{iz}^{\mathrm{DKM}} = \sigma_i\, V_{iz}$.

Next, we use the well-known Eckart–Young theorem of linear algebra (see, e. g., [50]), whereby the truncated SVD of matrix D obtained by setting to zero the $r - n_{\mathrm{c}}$ smallest singular values (i. e., by setting $\sigma_{n_{\mathrm{c}}+1} = \sigma_{n_{\mathrm{c}}+2} = \cdots = \sigma_r = 0$) is a matrix D_{approx} that provides the closest approximation of rank $\leq n_{\mathrm{c}}$ of the original matrix D, where by "closest" we mean that the Frobenius norm distance between the two matrices is minimal. The value of such norm, $\|D_{\mathrm{approx}} - D\|_{\mathrm{Fro}} = (\sum_{k=n_{\mathrm{c}}+1}^{r} \sigma_k^2)^{1/2}$, can be taken as a measure of the error introduced by approximating the full solution matrix $D_{jz} = \Lambda^{\mathrm{DKM}}_{\mathrm{DoD},jz}$ with its rank-n_{c} truncated SVD form

$$D_{jz}|_{\mathrm{approx}} = \Lambda^{\mathrm{DKM}}_{\mathrm{DoD},jz}|_{\mathrm{approx}} = \sum_{i=1}^{n_{\mathrm{c}}} U_{ji}\, \gamma_{iz}^{\mathrm{DKM}} \quad \text{or, equivalently,} \quad \mathbf{\Lambda}^{\mathrm{DKM}}_{\mathrm{DoD}}(z)|_{\mathrm{approx}} = \sum_{i=1}^{n_{\mathrm{c}}} \gamma_i^{\mathrm{DKM}}(z)\, \boldsymbol{u}_i. \tag{7}$$

As sketched in Fig. 1 (right), the evolution $\mathbf{\Lambda}^{\mathrm{DKM}}_{\mathrm{DoD}}(z)|_{\mathrm{approx}}$ of the approximate overall DoD vector is the projection of the evolution of the exact overall DoD vector $\mathbf{\Lambda}^{\mathrm{DKM}}_{\mathrm{DoD}}(z)$ onto the n_{c}-dimensional linear span of the first n_{c} vectors $\boldsymbol{u}_i$. The low-dimensional subspace span $(\{\boldsymbol{u}_i\}_{i=1}^{n_{\mathrm{c}}})$ where vectors $\mathbf{\Lambda}^{\mathrm{DKM}}_{\mathrm{DoD}}(z)|_{\mathrm{approx}}$ lie for every z is optimized in the sense that it minimizes the average distance between the evolutions of the approximate and the exact overall DoD vectors.

Therefore, the heart of the ASVDADD strategy for optimal automatic selection of RCCE constraints is to enforce the RCCE states to correspond to overall DoD vectors that remain within the subspace span $(\{\boldsymbol{u}_i\}_{i=1}^{n_c})$. This is readily done by assuming as constraints precisely the first n_c vectors $\boldsymbol{u}_i$, i. e., by setting (ASVDADD choice of RCCE constraints)

$$\boldsymbol{a}_i^{\mathrm{CE}} = \boldsymbol{u}_i \quad \text{or, equivalently,} \quad a_{ij}^{\mathrm{CE}} = U_{ji} \quad \text{for} \quad i = 1, \dots, n_c. \tag{8}$$

As a result, the RCCE computation is guaranteed to yield overall DoD vectors of the form

$$\Lambda_{\mathrm{DoD},jz}^{\mathrm{RCCE}} = \sum_{k=1}^{n_c} U_{jk}\, \gamma_{kz}^{\mathrm{CE}} = \sum_{i=1}^{n_c} \gamma_{iz}^{\mathrm{CE}}\, a_{ij}^{\mathrm{CE}} \quad \text{or, equivalently,} \quad \boldsymbol{\Lambda}_{\mathrm{DoD}}^{\mathrm{RCCE}}(z) = \sum_{i=1}^{n_c} \gamma_i^{\mathrm{CE}}(z)\, \boldsymbol{a}_i^{\mathrm{CE}}. \tag{9}$$

Interestingly, the r columns of the reduced SVD matrix $\boldsymbol{U}$ provide at once the entire set of optimal RCCE constraints, ordered in decreasing order of importance and hence ready for any choice of n_c. In MatLab this can be readily done using the command `[U,sigma,V] = svd(D,'econ')`. However, as already mentioned, the singular values provide the estimate $\mathcal{E}(n_c) = (\sum_{k=n_c+1}^{r} \sigma_k^2)^{1/2}$ of the error involved in the approximation $D \approx D_{\mathrm{approx}}$, which is obviously a decreasing function of n_c. Therefore, a more efficient algorithm could be to preset a threshold value $\mathcal{E}_{\max}$, compute just the r singular values of D (for example with the MatLab command `sigma = svd(D)`), and with them choose the smallest n_c such that $\mathcal{E}(n_c) < \mathcal{E}_{\max}$. Then, for example using the MatLab command `[U,sigma,V] = svds(D,k)` with `k` = n_c, one can more quickly compute just the truncated SVD, which is all that is needed to identify the n_c constraint vectors $\boldsymbol{u}_i$ for the preset level of approximation. The reader is referred to [34] for a detailed code of implementation of the ASVDADD algorithm in MatLab.

5 Rate equations for the constraint potentials

As done in [16, 31, 44, 45, 51, 52], the RCCE equations can be integrated more efficiently by rewriting them as rate equations for the elemental and constraint potentials. These are obtained by combining the species and energy balance equations, the kinetic equations, the ideal gas equation of state, and the linear combinations $c_i(\boldsymbol{N}) = \sum_{j=1}^{n_{sp}} a_{ij}^{\mathrm{CE}} N_j$ that define the values c_i of the constraints. As shown in Ref. [16], we obtain the following set of rate equations, where for convenience we use $\beta = 1/RT$ instead of the temperature and the notation $N_j = [N_j]V$ for the number of moles of species j, $u_{\boldsymbol{j}}$ and $c_{v\boldsymbol{j}}$ for the molar specific internal energy and heat capacity at constant volume of pure species j, and Φ for the viscous dissipation function (usually negligible):

$$\sum_{k=1}^{n_{el}} \dot{\gamma}_k^{\mathrm{EL}} \sum_{j=1}^{n_{sp}} a_{kj}^{\mathrm{EL}} N_j a_{ij}^{\mathrm{EL}} + \sum_{k=1}^{n_c} \dot{\gamma}_k^{\mathrm{CE}} \sum_{j=1}^{n_{sp}} a_{kj}^{\mathrm{CE}} N_j a_{ij}^{\mathrm{EL}} + \frac{\dot{\beta}}{\beta} \sum_{j=1}^{n_{sp}} N_j \beta u_{\boldsymbol{j}} a_{ij}^{\mathrm{EL}} = \frac{\dot{V}}{V} \sum_{j=1}^{n_{sp}} N_j a_{ij}^{\mathrm{EL}} + \sum_{j=1}^{n_{sp}} a_{ij}^{\mathrm{EL}} \dot{N}_j^{\rightarrow}$$
$$\text{for } i = 1, \dots, n_{el}, \tag{10}$$

$$\sum_{k=1}^{n_{el}} \dot{\gamma}_k^{\mathrm{EL}} \sum_{j=1}^{n_{sp}} a_{kj}^{\mathrm{EL}} N_j a_{ij}^{\mathrm{CE}} + \sum_{k=1}^{n_c} \dot{\gamma}_k^{\mathrm{CE}} \sum_{j=1}^{n_{sp}} a_{kj}^{\mathrm{CE}} N_j a_{ij}^{\mathrm{CE}} + \frac{\dot{\beta}}{\beta} \sum_{j=1}^{n_{sp}} N_j \beta u_{\boldsymbol{j}} a_{ij}^{\mathrm{CE}} = \frac{\dot{V}}{V} \sum_{j=1}^{n_{sp}} N_j a_{ij}^{\mathrm{CE}} + \sum_{j=1}^{n_{sp}} a_{ij}^{\mathrm{CE}} \dot{N}_j^{\rightarrow} - \dot{c}_{i,\mathrm{chem}}(\beta, p, \boldsymbol{N})$$
$$\text{for } i = 1, \dots, n_c, \tag{11}$$

$$\sum_{k=1}^{n_c} \dot{\gamma}_k^{\mathrm{EL}} \sum_{j=1}^{n_{sp}} a_{kj}^{\mathrm{EL}} N_j \beta u_{\boldsymbol{j}} + \sum_{k=1}^{n_c} \dot{\gamma}_k^{\mathrm{CE}} \sum_{j=1}^{n_{sp}} a_{kj}^{\mathrm{CE}} N_j \beta u_{\boldsymbol{j}} + \frac{\dot{\beta}}{\beta} \sum_{j=1}^{n_{sp}} N_j \left(\beta^2 u_{\boldsymbol{j}}^2 = \frac{c_{v\boldsymbol{j}}}{R} \right) + \frac{\dot{V}}{V} \sum_{j=1}^{n_{sp}} N_j \beta u_{\boldsymbol{j}} + \beta \dot{E}^{\rightarrow} + \beta p\, \dot{V} - \beta V \Phi, \tag{12}$$

$$\sum_{k=1}^{n_c} \dot{\gamma}_k^{\mathrm{EL}} \sum_{j=1}^{n_{sp}} a_{kj}^{\mathrm{EL}} N_j + \sum_{k=1}^{n_c} \dot{\gamma}_k^{\mathrm{CE}} \sum_{j=1}^{n_{sp}} a_{kj}^{\mathrm{CE}} N_j + \frac{\dot{\beta}}{\beta} \sum_{j=1}^{n_{sp}} N_j \left(\beta u_{\boldsymbol{j}} + 1 \right) + \frac{\dot{p}}{p} \sum_{j=1}^{n_{sp}} N_j = 0, \tag{13}$$

where $\dot{N}_j^{\rightarrow}$ and $\dot{E}^{\rightarrow}$ denote the species and energy transport rates (positive if outgoing), the bottleneck source terms are

$$\dot{c}_{i,\mathrm{chem}}(\beta, p, \boldsymbol{N}) = V \sum_{\ell=1}^{n_r} \Big(\sum_{m=1}^{n_{sp}} a_{im}^{\mathrm{CE}} \nu_{m\ell} \Big) \left[\frac{k_\ell^+(\beta, p)}{V^{\nu_\ell^+}} \prod_{j=1}^{n_{sp}} (N_j)^{\nu_{j\ell}^+} - \frac{k_\ell^-(\beta, p)}{V^{\nu_\ell^-}} \prod_{j=1}^{n_{sp}} (N_j)^{\nu_{j\ell}^-} \right], \tag{14}$$

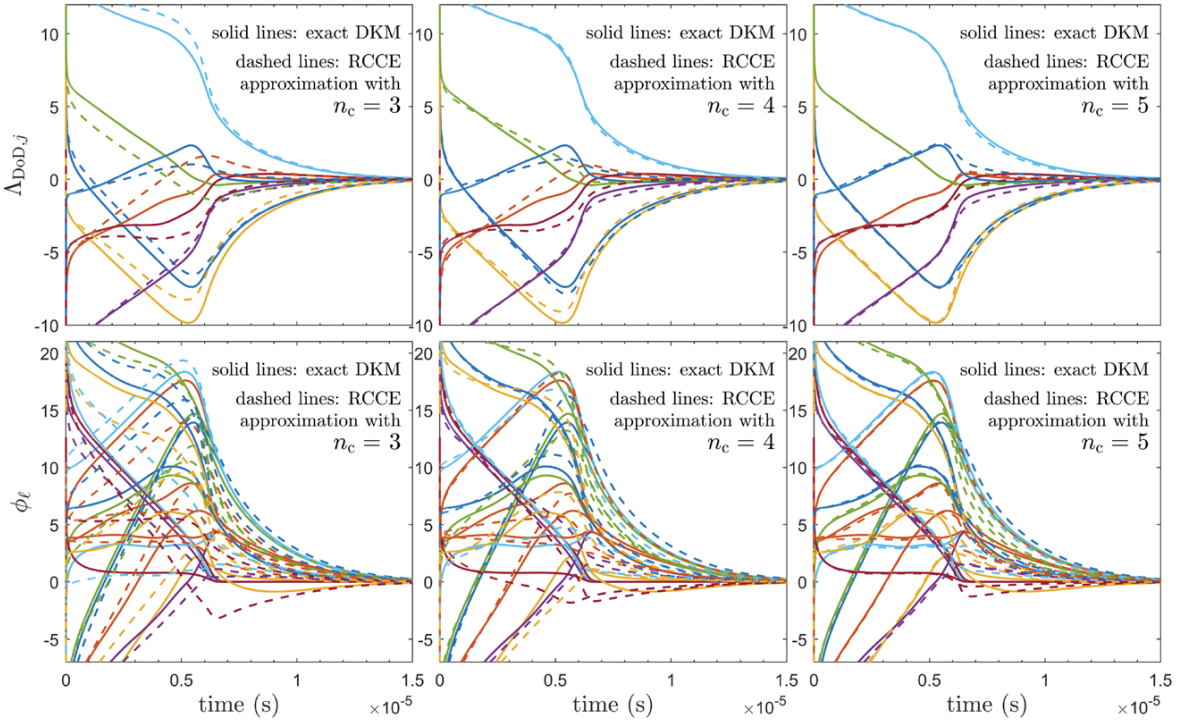

Figure 2: Close-up of the final stage of the ignition process of a homogeneous stoichiometric mixture of hydrogen and oxygen initially at 1 atm and 1500 K. **Upper plots:** Comparisons of the time evolutions of the 8 components $\Lambda_{\mathrm{DoD},j}$ of vectors $\mathbf{\Lambda}^{\mathrm{DKM}}_{\mathrm{DoD}}(t)$ (solid lines) and $\mathbf{\Lambda}^{\mathrm{RCCE}}_{\mathrm{DoD}}(t)$ (dashed lines) for $n_c = 3,\ 4,\ 5$ ASVDADD constraints. **Lower plots:** Comparisons of the time evolutions of the degrees of disequilibrium, ϕ_ℓ, of the 24 reactions in detailed kinetic model.

and the composition is that given by eq. (1), i. e.,

$$N_j = \beta p V X_j = \exp\Big(- g_{j,\mathrm{pure}}(\beta,p)\beta - \sum_{i=1}^{n_{\mathrm{el}}} \gamma_i^{\mathrm{EL}} a_{ij}^{\mathrm{EL}} - \sum_{i=1}^{n_c} \gamma_i^{\mathrm{CE}} a_{ij}^{\mathrm{CE}} \Big) \qquad \text{for } j = 1,\dots,n_{\mathrm{sp}}. \tag{15}$$

The above $n_{\mathrm{el}} + n_{\mathrm{nc}} + 2$ implicit differential equations together with the n_{sp} eqs. (15) can be solved for given values of $\dot{E}^{\rightarrow}$, $V(t)$, and the $\dot{N}_j^{\rightarrow}$, to yield the $n_{\mathrm{sp}}+2$ state variables $\beta(t)$, $p(t)$, and $N_j(t)$ and the $n_{\mathrm{el}}+n_c$ constraint potentials $\gamma_i^{\mathrm{EL}}(t)$ and $\gamma_i^{\mathrm{CE}}(t)$.

It is important to notice that in eqs. (14) only the chemical reactions that are not equilibrated contribute to $\dot{c}_{i,\mathrm{chem}}$, i. e., only those for which $b_{i\ell}^{\mathrm{CE}} = \sum_{m=1}^{n_{\mathrm{sp}}} a_{im}^{\mathrm{CE}} \nu_{m\ell} \neq 0$. In fact, from eqs. (3), (6), and (8) we write

$$\phi_\ell^{\mathrm{DKM}} = \sum_{j=1}^{n_{\mathrm{sp}}} \Lambda_{\mathrm{DoD},jz}^{\mathrm{DKM}} \nu_{j\ell} = \sum_{j=1}^{n_{\mathrm{sp}}} \nu_{j\ell} \sum_{i=1}^{r} U_{ji}\, \sigma_i\, V_{iz} = \sum_{i=1}^{r} \Big(\sum_{j=1}^{n_{\mathrm{sp}}} \nu_{j\ell} U_{ji} \Big) \gamma_{iz}^{\mathrm{DKM}} = \sum_{i=1}^{r} b_{i\ell}\, \gamma_{iz}^{\mathrm{DKM}}, \tag{16}$$

where we defined $b_{i\ell} = \sum_{j=1}^{n_{\mathrm{sp}}} \nu_{j\ell} U_{ji}$, which shows that within the RCCE approximation – whereby we set to zero the singular values $\sigma_{n_c+1} = \sigma_{n_c+2} = \cdots = \sigma_r = 0$ and we set $a_{ij}^{\mathrm{CE}} = U_{ji}$ for $i = 1,\dots,n_c$ – the DoDs are given by

$$\phi_\ell^{\mathrm{RCCE}} = \sum_{i=1}^{n_c} b_{i\ell}^{\mathrm{CE}}\, \sigma_i\, V_{iz} = \sum_{i=1}^{n_c} b_{i\ell}^{\mathrm{CE}}\, \gamma_{iz}^{\mathrm{CE}} \tag{17}$$

and therefore the reactions that contribute to $\dot{c}_{i,\mathrm{chem}}$, those with $b_{i\ell}^{\mathrm{CE}} \neq 0$, are those with a nonzero DoD.

To illustrate the results of integrating the above equations we consider the 8 species/24 reactions hydrogen/oxygen detailed kinetic mechanism considered in [34, 51] and the problem of predicting the ignition delay of a homogeneous stoichiometric mixture of H_2 and O_2 initially at 1 atm and 1500 K. The upper plots in Fig. 2 show comparisons of the time evolutions of the 8 components $\Lambda_{\mathrm{DoD},j}$ of vectors $\mathbf{\Lambda}^{\mathrm{DKM}}_{\mathrm{DoD}}(t)$ (solid lines)

and $\mathbf{\Lambda}_{\mathrm{DoD}}^{\mathrm{RCCE}}(t)$ (dashed lines) for $n_c = 3, 4, 5$ constraints selected by means of the ASVDADD method. From these, through eq. (3), we compute the lower plots in Fig. 2, showing the time evolutions of the ϕ_ℓs of the 24 reactions. The figure involves a close-up of the final stage of the ignition process and shows the consistent improvement of the RCCE approximation by increasing the number of ASVDADD constraints.

6 Conclusions

The ASVDADD algorithm identifies a full sequence of RCCE constraints that characterize the kinetic bottlenecks effectively rate-controlling the underlying DKM in the chosen range of conditions as it emerges from DoD analysis of a probe full DKM computation. The algorithm automatically ranks the candidate constraints in terms of their relative contributions to the average overall degree of disequilibrium along the probe DKM computation. These features make the algorithm suitable for adaptive or tabulation strategies and therefore opens up the advantages of the RCCE method to effective implementations in the context of CFD simulation along the lines suggested in [26, 29].

The ASVDADD strategy for systematic RCCE constraint identification is based on analyzing how the degrees of disequilibrium of the chemical reactions behave in a full DKM probe simulation. Geometrically, the procedure identifies a hierarchy of subspaces of the reactive space that have decreasing dimensionality and are at minimal average distance from the exact evolution of the overall DoD vector.

The effectiveness and robustness of the methodology have already been demonstrated in [34, 44, 45] for different combustion systems. The excellent performance of the ASVDADD constraints confirms the conclusion that the new algorithm essentially resolves the difficulties that have prevented the RCCE method from a more widespread use in systematic model order reduction of detailed combustion kinetic models of hydrocarbon fuels.

We hope that future work will show that the same model order reduction strategy is suitable and can find useful applications also in model reduction of complex biochemical kinetic schemes (such as in [21, 22, 23, 53, 54]), complex fluid structure interactions such as turbulence generated noise [55, 56], as well as natural extensions in the more general frameworks of nonequilibrium thermodynamics modeling (such as in [35, 36, 37, 38, 39, 40, 41, 57, 58]).

References

[1] S. Vajda, P. Valko, and T. Turanyi, Principal component analysis of kinetic models, *Int. J. Chem. Kinet.* **17** (1985), 55–81.
[2] S. H. Lam and D. A. Goussis, Understanding complex chemical kinetics with computational singular perturbation, *Symp., Int., Combust.* **22** (1988), 931–941.
[3] S. J. Fraser, The steady state and equilibrium approximations: A geometrical picture, *J. Chem. Phys.* **88** (1988), 4732–4738.
[4] R. Law, M. Metghalchi, and J. C. Keck, Rate-controlled constrained equilibrium calculation of ignition delay times in hydrogen-oxygen mixtures, *Symp., Int., Combust.* **22** (1989), 1705–1713.
[5] J. C. Keck, Rate-controlled constrained-equilibrium theory of chemical reactions in complex systems, *Prog. Energy Combust. Sci.* **16** (1990), 125–154.
[6] M. R. Roussel and S. J. Fraser, On the geometry of transient relaxation, *J. Chem. Phys.* **94** (1991), 7106–7113.
[7] U. Maas and S. B. Pope, Simplifying chemical kinetics – Intrinsic low dimensional manifolds in composition space, *Combust. Flame* **88** (1992), 239–264.
[8] G. Li, A. S. Tomlin, H. Rabitz, and J. Tóth, Determination of approximate lumping schemes by a singular perturbation method, *J. Chem. Phys.* **99** (1993), 3562–3574.
[9] S. Singh, J. M. Powers, and S. Paolucci, On slow manifolds of chemically reactive systems, *J. Chem. Phys.* **117** (2002), 1482–1496.
[10] E. L. Haseltine and J. B. Rawlings, Approximate simulation of coupled fast and slow reactions for stochastic chemical kinetic, *J. Chem. Phys.* **117** (2002), 6959–6969.
[11] A. N. Gorban and I. V. Karlin, Method of invariant manifold for chemical kinetics, *Chem. Eng. Sci.* **58** (2003), 4751–4768.
[12] D. Lebiedz, Computing minimal entropy production trajectories: An approach to model reduction in chemical kinetics, *J. Chem. Phys.* **120** (2004), 6890–6897.

[13] M. Valorani, F. Creta, D. A. Goussis, J. C. Lee, and H. N. Najm, An automatic procedure for the simplification of chemical kinetic mechanisms based on CSP, *Combust. Flame* **146** (2006), 29–51.
[14] E. Chiavazzo, A. N. Gorban, and I. V. Karlin, Comparison of invariant manifolds for model reduction in chemical kinetics, *Commun. Comput. Phys.* **2** (2007), 964–992.
[15] A. N. Al-Khateeb, J. M. Powers, S. Paolucci, A. J. Sommese, J. A. Diller, J. D. Hauenstein, et al.,One-dimensional slow invariant manifolds for spatially homogenous reactive systems, *J. Chem. Phys.* **131** (2009), 024118.
[16] G. P. Beretta, J. C. Keck, M. Janbozorgi, and H. Metghalchi, The rate-controlled constrained-equilibrium approach to far-from-local-equilibrium thermodynamics, *Entropy* **14** (2012), 92–130.
[17] E. P. Gyftopoulos and G. P. Beretta, Entropy generation rate in a chemically reacting system, *J. Energy Resour. Technol.* **115** (1993), 208–212.
[18] J. C. Keck and D. Gillespie, Rate-controlled partial-equilibrium method for treating reacting gas mixtures, *Combust. Flame* **17** (1971), 237–241.
[19] J. C. Keck, Rate-controlled constrained equilibrium method for treating reactions in complex systems, in: R. D. Levine, M. Tribus (Eds.), *The Maximum Entropy Formalism*, MIT Press, Cambridge, MA, 1979, pp. 219–245. Available online at www.jameskeckcollectedworks.org/.
[20] G. P. Beretta and J. C. Keck, The constrained-equilibrium approach to nonequilibrium dynamics, in: R. A. Gaggioli (Ed.), *Second Law Analysis and Modeling*, ASME Book H0341C-AES, Vol. 3, ASME, New York, 1986, pp. 135–139. Available online at www.jameskeckcollectedworks.org/.
[21] K. C. Chen, A. Csikász-Nagy, B. Gyorffy, J. Val, B. Novák, and J. J. Tyson, Kinetic analysis of a molecular model of the budding yeast cell cycle, *Mol. Biol. Cell* **11** (2000), 369–391.
[22] A. Lovrics, A. Csikász-Nagy, I. G. Zsély, J. Zádor, T. Turányi, and B. Novák, Time scale and dimension analysis of a budding yeast cell cycle model, *BMC Bioinform.* **7** (2006), 494.
[23] I. Surovtsova, N. Simus, T. Lorenz, A. König, S. Sahle, and U. Kummer, Accessible methods for the dynamic time-scale decomposition of biochemical systems, *Bioinformatics* **25** (2009), 2816–2823.
[24] A. I. Karpov, Minimal entropy production as an approach to the prediction of the stationary rate of flame propagation, *J. Non-Equilib. Thermodyn.* **17** (1992), 1–10.
[25] V. Yousefian, A rate-controlled constrained-equilibrium thermochemistry algorithm for complex reacting systems, Combust. Flame **115** (1998), 66–80.
[26] Q. Tang and S. B. Pope, Implementation of combustion chemistry by in situ adaptive tabulation of rate-controlled constrained equilibrium manifolds, *Proc. Combust. Inst.* **29** (2002), 1411–1417.
[27] Q. Tang and S. B. Pope, A more accurate projection in the rate-controlled constrained equilibrium method for dimension reduction of combustion chemistry, *Combust. Theory Model.* **8** (2004), 255–279.
[28] S. Rigopoulos and T. Løvås, A LOI-RCCE methodology for reducing chemical kinetics, with application to laminar premixed flames, *Proc. Combust. Inst.* **32** (2009), 569–576.
[29] T. Løvås, S. Navarro-Martinez, and S. Rigopoulos, On adaptively reduced chemistry in large eddy simulations, *Proc. Combust. Inst.* **33** (2011), 1339–1346.
[30] V. Hiremath and S. B. Pope, A study of the rate-controlled constrained-equilibrium dimension reduction method and its different implementations, *Combust. Theory Model.* **17** (2013), 260–293.
[31] F. Hadi and M. R. H. Sheikhi, A comparison of constraint and constraint potential forms of the Rate-Controlled Constraint-Equilibrium method, *J. Energy Resour. Technol.* **138** (2015), 022202.
[32] F. Hadi, M. Janbozorgi, M. R. H. Sheikhi, and H. Metghalchi, A study of interactions between mixing and chemical reaction using the Rate-Controlled Constrained-Equilibrium method, *J. Non-Equilib. Thermodyn.* **41** (2016), 257–278.
[33] F. Hadi, V. Yousefian, M. R. H. Sheikhi, and H. Metghalchi, Time scale analysis for Rate-Controlled Constrained-Equilibrium constraint selection, in: *Proceedings of the 10th U.S. National Combustion Meeting, Eastern States Section of the Combustion Institute*, College Park, Maryland, April 23–26, 2017, 1–6.
[34] G. P. Beretta, M. Janbozorgi, and H. Metghalchi, Degree of Disequilibrium Analysis for Automatic Selection of Kinetic Constraints in the Rate-Controlled Constrained-Equilibrium Method, *Combust. Flame* **168** (2016), 342–364.
[35] H. C. Ottinger, General projection operator formalism for the dynamics and thermodynamics of complex fluids, *Phys. Rev. E* **57** (2015), 1416–1420.
[36] G. P. Beretta, Steepest Entropy Ascent model for far-non-equilibrium thermodynamics. Unified implementation of the Maximum Entropy Production Principle, *Phys. Rev. E* **90** (2014), 042113.
[37] A. Montefusco, F. Consonni, and G. P. Beretta, Essential equivalence of the general equation for the nonequilibrium reversible-irreversible coupling (GENERIC) and steepest-entropy-ascent models of dissipation for nonequilibrium thermodynamics, *Phys. Rev. E* **91** (2015), 042138.
[38] S. Cano-Andrade, G. P. Beretta, and M. R. von Spakovsky, Steepest-entropy-ascent quantum thermodynamic modeling of decoherence in two different microscopic composite systems, *Phys. Rev. A* **91** (2015), 013848.
[39] G. Li and M. R. von Spakovsky, Steepest-entropy-ascent quantum thermodynamic modeling of the relaxation process of isolated chemically reactive systems using density of states and the concept of hypoequilibrium state, *Phys. Rev. E* **93** (2016), 012137.

[40] G. Lebon, D. Jou, and M. Grmela, Extended reversible and irreversible thermodynamics: A Hamiltonian approach with application to heat waves, *J. Non-Equilib. Thermodyn.* **42** (2017), 153–168.
[41] G. Li, M. R. von Spakovsky, and C. Hin, Steepest entropy ascent quantum thermodynamic model of electron and phonon transport, *Phys. Rev. B* **97** (2018), 024308.
[42] G. P. Beretta and E. P. Gyftopoulos, What is a chemical equilibrium state? J. Energy Resour. Technol. **137** (2015), 021008.
[43] G. P. Beretta and J. C. Keck, Energy and entropy balances in a combustion chamber. Analytical solution, *Combust. Sci. Technol.* **30** (1983), 19–29.
[44] G. P. Beretta, M. Janbozorgi, and H. Metghalchi, Use of degree of disequilibrium analysis to select kinetic constraints for the Rate-Controlled Constrained-Equilibrium (RCCE) method, in: *Proceedings of ECOS 2015 – The 28th International Conference On Efficiency, Cost, Optimization, Simulation and Environmental Impact of Energy Systems*, Pau, France, June 30–July 3, 2015. Available online at www.gianpaoloberetta.info/.
[45] L. Rivadossi and G. P. Beretta, Validation of the ASVDADD constraint selection algorithm for effective RCCE modeling of natural gas ignition in air, in: *Proceedings of IMECE2016 – the ASME 2016 International Mechanical Engineering Congress and Exposition*, November 11–17, 2016, Phoenix, Arizona, USA – paper IMECE2016-65323. Available online at www.gianpaoloberetta.info/ https://doi.org/10.1115/IMECE2016-65323.
[46] G. P. Beretta, Nonlinear quantum evolution equations to model irreversible adiabatic relaxation with maximal entropy production and other nonunitary processes, *Rep. Math. Phys.* **64** (2009), 139–168.
[47] M. Valorani, D. A. Goussis, F. Creta, and H. N. Najm, Higher order corrections in the approximation of inertial manifolds and the construction of simplified problems with the CSP method, *J. Comput. Phys.* **209** (2005), 754–786.
[48] D. Lebiedz, V. Reinhardt, and J. Siehr, Minimal curvature trajectories: Riemannian geometry concepts for slow manifold computation in chemical kinetics, *J. Comp. Physiol.* **229** (2010), 6512–6533.
[49] D. Lebiedz, J. Siehr, and J. Unger, A variational principle for computing slow invariant manifolds in dissipative dynamical systems, *SIAM J. Sci. Comput.* **33** (2011), 703–720.
[50] C. D. Martin and M. A. Porter, The extraordinary SVD, *Am. Math. Mon.* **119** (2012), 838–851.
[51] M. Janbozorgi and H. Metghalchi, Rate-Controlled Constrained-Equilibrium Modeling of H-O Reacting Nozzle Flow, *J. Propuls. Power* **28** (2012), 677–684.
[52] L. Rivadossi and G. P. Beretta, Validation of the ASVDADD constraint selection algorithm for effective RCCE modeling of natural gas ignition in air, *J. Energy Resour. Technol.* **140** (2018), 052201.
[53] P. D. Kourdis, R. Steuer, and D. A. Goussis, Physical understanding of complex multiscale biochemical models via algorithmic simplification: Glycolysis in saccharomyces cerevisiae, *Physica D* **239** (2010), 1798–1817.
[54] V. Damioli, G. P. Beretta, A. Salvadori, C. Ravelli, and S. Mitola, Multi-physics interactions drive VEGFR2 relocation on endothelial cells, *Scientific Reports* **7** (2017), 16700.
[55] E. A. Piana, S. Uberti, A. Copeta, B. Motyl, and G. Baronio, An integrated acoustic–mechanical development method for off-road motorcycle silencers: from design to sound quality test, *Int. J. Interact. Des. Manuf.* (2018). https://doi.org/10.1007/s12008-018-0464-x.
[56] E. A. Piana, B. Grassi, F. Bianchi, and C. Pedrotti, Hydraulic balancing strategies: A case-study of radiator-based central heatig systems, *Building Serv. Eng. Res. Technol.* (2018). https://doi.org/10.1177/0143624417752830.
[57] G. P. Beretta, Modeling non-equilibrium dynamics of a discrete probability distribution: General rate equation for maximal entropy generation in a maximum-entropy landscape with time-dependent constraints, *Entropy* **10** (2008), 160–182.
[58] L. M. Martyushev and V. D. Seleznev, Maximum entropy production: application to crystal growth and chemical kinetics, *Current Opinion in Chemical Engineering* **7** (2015), 23–31.